

Effective light trapping enhancement by plasmonic Ag nanoparticles on silicon pyramid surface

Han Dai,¹ Meicheng Li,^{1,3,*} Yingfeng Li,¹ Hang Yu,¹ Fan Bai,² and Xiaofeng Ren²

¹State Key Laboratory of Alternate Electrical Power System with Renewable Energy Sources, North China Electric Power University, Beijing, 102206, China

²School of Materials Science and Engineering, Harbin Institute of Technology, Harbin, 165001, China

³Su Zhou Institute, North China Electric Power University, Suzhou, 215123, China

*mcli@ncepu.edu.cn

Abstract: Plasmonic Ag nanoparticles were deposited on the silicon pyramid structures to further reduce surface reflectance. Compared with the bare silicon pyramid surface, a dramatic reflectance reduction around 380 nm was observed and the weighted average surface reflectance from 300 nm to 1100 nm could be reduced about 3.4%. By a series of designed experiments combined with Mie theory calculations, the influences of the size, shape and density distribution of Ag nanoparticles on the surface reflectance reduction were investigated in detail. This study shows a practicable method to improve light trapping for the application to solar cells.

©2012 Optical Society of America

OCIS codes: (240.0240) Optics at surfaces; (240.6680) Surface plasmons; (290.4020) Mie theory.

References and links

1. C. Eminian, F. J. Haug, O. Cubero, X. Niquille, and C. Ballif, "Photocurrent enhancement in thin film amorphous silicon solar cells with silver nanoparticles," *Prog. Photovolt. Res. Appl.* **19**(3), 260–265 (2011).
2. J. K. Mapel, M. Singh, M. A. Baldo, and K. Celebi, "Plasmonic excitation of organic double heterostructure solar cells," *Appl. Phys. Lett.* **90**(12), 121102 (2007).
3. K. Nakayama, K. Tanabe, and H. A. Atwater, "Plasmonic nanoparticle enhanced light absorption in GaAs solar cells," *Appl. Phys. Lett.* **93**(12), 121904 (2008).
4. S. Mokkaapati, F. J. Beck, R. de Waele, A. Polman, and K. R. Catchpole, "Resonant nano-antennas for light trapping in plasmonic solar cells," *J. Phys. D Appl. Phys.* **44**(18), 185101 (2011).
5. S. Pillai, K. R. Catchpole, T. Trupke, and M. A. Green, "Surface plasmon enhanced silicon solar cells," *J. Appl. Phys.* **101**(9), 093105 (2007).
6. M. Rycenga, C. M. Cobley, J. Zeng, W. Li, C. H. Moran, Q. Zhang, D. Qin, and Y. Xia, "Controlling the synthesis and assembly of silver nanostructures for Plasmonic Applications," *Chem. Rev.* **111**(6), 3669–3712 (2011).
7. D. Derkacs, S. H. Lim, P. Matheu, W. Mar, and E. T. Yu, "Improved performance of amorphous silicon solar cells via scattering from surface plasmon polaritons in nearby metallic nanoparticles," *Appl. Phys. Lett.* **89**(9), 093103 (2006).
8. E. D. Palik, *Handbook of Optical Constants of Solids* (Academic, 1985).
9. C. Rockstuhl, S. Fahr, and F. Lederer, "Absorption enhancement in solar cells by localized plasmon polaritons," *J. Appl. Phys.* **104**(12), 123102 (2008).
10. P. A. Ragip, W. Justin, B. Edward, L. John, and B. L. Mark, "Design of plasmonic thin-film solar cells with broadband absorption enhancements," *Adv. Mater. (Deerfield Beach Fla.)* **21**, 1–6 (2009).
11. N. C. Panoiu and R. M. Osgood, Jr., "Enhanced optical absorption for photovoltaics via excitation of waveguide and plasmon-polariton modes," *Opt. Lett.* **32**(19), 2825–2827 (2007).
12. K. L. Kelly, E. Coronado, L. L. Zhao, and G. C. Schatz, "The optical properties of metal nanoparticles: The influence of size, shape, and dielectric environment," *J. Phys. Chem. B* **107**(3), 668–677 (2003).
13. M. C. Carotta, M. Merli, L. Passari, D. Palmeri, G. Martinelli, and R. Van Steenwinkel, "Effect of Thickness and surface treatment on silicon water reflectance," *Sol. Energy Mater. Sol. Cells* **27**(3), 265–272 (1992).
14. A. W. Smith and A. Rohatgi, "Ray tracing analysis of the inverted pyramid texturing geometry for high efficiency silicon solar cells," *Sol. Energy Mater. Sol. Cells* **29**(1), 37–49 (1993).

15. Z. Xin, W. Lei, and Y. D. Ren, "Investigations of random pyramid texture on the surface of single-crystalline silicon for solar cells," *Proceedings of ISES World Congress* **4**, 1126–1130 (2007).
 16. T. L. Temple, G. D. K. Mahanama, H. S. Reehal, and D. M. Bagnall, "Influence of localized surface plasmon excitation in silver nanoparticles on the performance of silicon solar cells," *Sol. Energy Mater. Sol. Cells* **93**(11), 1978–1985 (2009).
 17. C. F. Bohren and D. R. Huffman, *Absorption and Scattering of Light by Small Particles* (Wiley-Interscience, 1983).
 18. K. R. Catchpole and A. Polman, "Design principles for particle plasmon enhanced solar cells," *Appl. Phys. Lett.* **93**(19), 191113 (2008).
 19. H. Qian, Z. X. Dan, and W. Shuo, "Research on fabricating functional optical Ag thin films and optical properties," *Acta. Phys. Sin. (Overseas Ed)* **58**, 2731–2736 (2009).
 20. U. Kreibig and M. Vollmer, *Optical properties of metal clusters* (Springer-Verlag, 1995).
 21. B. Soller, *The Interaction Between Metal Nanoparticle Resonances and Optical Frequency Surface Waves* (University of Rochester, 2002).
-

1. Introduction

Currently, local surface plasmon (LSP) in metallic nanoparticles currently has been widely exploited for a variety of solar cells including thin layer, organic and Si based solar cells [1–5]. The common material choices are Ag and Au, owing to their excellent light trapping ability [6,7]. And among them, Ag is much better for its cheaper cost and lower absorption losses in the visible spectrum [8]. Several detail investigations have been done to study the light trapping abilities of Ag nanoparticles with different sizes, shapes and local dielectric environment [9]. However, all these works were carried out on Ag nanoparticles deposited on flat surface, in which, the back scattering could not be collected by substrates and large part of rays scattered back into air [10–12].

In this work, taking advantage of both the effective back scattering collection ability of silicon pyramids surface [13–15] and the light trapping abilities of the metal nanoparticles, a new structure that deposit Ag nanoparticles on silicon pyramid surface was fabricated to further enhance the light trapping efficiency. Then, the influences of the size, shape and density distribution of Ag nanoparticles on the surface reflectance reduction were investigated in detail. To reveal the reflectance reduction mechanism of this structure, theoretical simulations based on Mie theory were also carried out [16]. This study shows a practicable method to reduce the surface reflectance of silicon pyramid surface.

2. Experiment methods and simulation sets

In our experiments, the one-side polished p-type Si (100) wafers with thickness around 0.5 mm were employed. The silicon pyramid surface was fabricated by exposing these samples into an etching solution, which is composited by NaOH (3wt%), IPA (8voltage%) and deionized water [17], at 80 °C for 40 min. Ag nanoparticles were fabricated on silicon pyramid surface through sputter-anneal process. And the sizes, shapes and densities of Ag nanoparticles were controlled by varying sputter time, current and annealed conditions. In our experiments, all sputtering processes were sustained 30s with the sputter current range from 20 mA to 35 mA to deposited Ag thin layers onto the silicon pyramid surface. And the annealing processes were carried out in nitrogen at 200 °C for 1.5h to coalesce the flat layers together to form nanoparticles with different shapes, sizes, densities and density distributions.

The sputtering of Ag layers was completed by Quorum Q150TS, the surface reflectance (300-1100 nm) were measured by Solar Cell QE/IPCE Measurement System. This system is a common experiment set-up used for measuring quantum efficiency, photon-to-electron conversion efficiency of solar cells and surface reflectance of photoelectric materials by monochromatic incident. The main specifications of the system are expressed as following: Wavelength range is 0.3-1.10 μm and measurement error is 0.2 nm, FWHM (Full Wave at Half Maximum) is 0.1 nm and reflectance measurement error is 0.1%. And the shape, size, density and size distribution of Ag nanoparticles of these samples were characterized by Scanning electron microscopy (SEM).

For the calculations, a model was designed as shown in Fig. 1. to describe the structure obtained in our experiments. The height of each pyramid is 3.266 μm , and the distribution of Ag nanoparticles is evenly deposited on them. In the following numerical calculations, these pyramids were divided into 10 layers from bottom to top, and the area of the nth layer can be expressed as:

$$l_n = 4 - \frac{2 \cdot \Delta h}{\sqrt{3}} (n-1). \quad (1)$$

where l_n is the nth layer area of the lateral surface, and n is the layer number.

To simplify our model, the incident light is assumed perpendicular to the pyramid bottom in our model, as shown in Fig. 1. And from this assumption, the effective scattering angle θ_n of the nth layer, which represents the arrangement of back scattering light collected by pyramids B, was deduced as:

$$\theta_n = \text{Arc cos}\left(\frac{(n-1/2)\Delta h - \cos(70.6^\circ) \cdot h}{\sqrt{n-1/2)^2 \Delta h^2 + h^2 - 2 \cos(70.6^\circ) \cdot h \times (n-1/2)\Delta h}}\right). \quad (2)$$

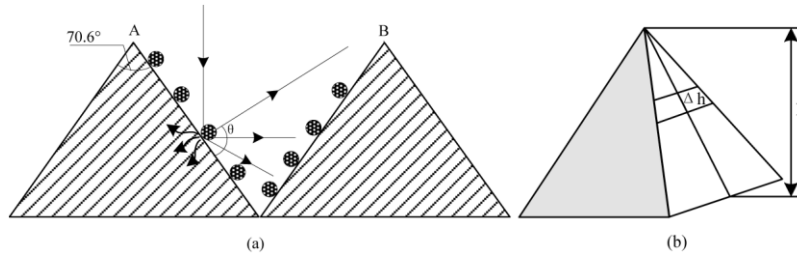


Fig. 1. Surface reflectance calculation model of Ag nanoparticles deposited on the pyramids (a) Scattering model of Ag particles deposited on pyramids. (b) The dividing methods for single pyramid.

Applying Mie theory to our model, we assume that Ag spherical nanoparticles in a matrix with an averaged dielectric function in between the vacuum value and that of the support material Si. Considering these assumptions, the scattering cross section C_{sca} and extinction cross section C_{ext} of Ag nanoparticles can be expressed as [13]:

$$C_{sca} = \frac{2}{x^2} \sum_{n=1}^{\infty} (2n+1) (|a_n|^2 + |b_n|^2). \quad (3)$$

$$C_{ext} = \frac{2}{x^2} \sum_{n=1}^{\infty} (2n+1) \text{Re}(a_n + b_n). \quad (4)$$

In our model, the parallel and perpendicular polarizations incident light were divided into the equivalent two parts. And the expression of the amplitude-scattering matrix elements of parallel and perpendicular polarizations of spherical nanoparticles can be depicted by:

$$S_1(\cos(\theta)) = \sum_n \frac{2n+1}{n(n+1)} (a_n \sigma_n + b_n \tau_n). \quad (5)$$

$$S_2(\cos(\theta)) = \sum_n \frac{2n+1}{n(n+1)} (a_n \tau_n + b_n \sigma_n). \quad (6)$$

In these expressions, a_n and b_n are the scattering coefficients of the nth scattering electromagnetic mode. In Eq. (3). and Eq. (4)., $x = 2\pi Na/\lambda$, a is the size of particle and N is averaged dielectric function in between the vacuum value and that of the support material. In

Eq. (5). and Eq. (6)., S_1 , S_2 represent parallel and polarization of amplitude scattering distribution. σ_n and τ_n represent the angle-dependent functions of the n th mode. θ is the scattering angle has a range $0 < \theta < \pi$, and λ is wavelength of the incidence light.

By applying Mie theory to this model, the forward-scattering light scattered into pyramid A was obtained as following:

$$\eta_A^{forward} = \frac{I_0}{2} \cdot \frac{C_{sca} \cdot l_n}{C_{ext} \cdot l} \left(2 \cdot \int_0^{35.3^\circ} |S_j(\theta)|^2 d\theta + \int_{35.3^\circ}^{144.7^\circ} |S_j(\theta)|^2 d\theta \right). \quad (7)$$

And the backscattered light collected by pyramid B could be expressed as:

$$\eta_A^{back} = \frac{I_0}{2} \cdot \frac{C_{sca} \cdot l_n}{C_{ext} \cdot l} \int_{35.3^\circ}^{35.3^\circ - \theta_n} |S_j(\theta)|^2 d\theta. \quad (8)$$

where I_0 is the intensity of total incident light, and l is the area of the lateral surface. The scattering efficiency of pyramid B can be given in the same way.

Other assumptions in our deduction are that the light absorption of Ag nanoparticles is neglected as its low value [18], all scattered lights from pyramid A to pyramid B by Ag nanoparticles are parallel to the bottom of the pyramids for simple, and only twice reflections are considered. Based on these assumptions, the final surface reflectance was obtained by combing calculation results of scattering mount of parallel and perpendicular polarizations, which can be expressed as follow:

$$ref_{total} = 1 - \eta_A^{forward} - \eta_B^{forward}. \quad (9)$$

where, $\eta_A^{forward}$ and $\eta_B^{forward}$ represent the forward scattering of pyramid A and pyramid B respectively.

4. Results and discussion

As the coactions of the plasmon enhancement of Ag nanoparticles and the backscattering collection effect of silicon pyramid surface, the reflectance of the new structure with Ag nanoparticles on silicon pyramid shows an obviously reduction. Figure 2 shows the anti-reflectance curves of the new structure 35% covered by spherical Ag nanoparticles, whose average radii are around 68 nm. Compared with that of the bare silicon pyramid surface, a dramatic reflectance reduction around 380 nm was observed and the weighted average surface reflectance from 300 nm to 1100 nm reduced about 3.4%.

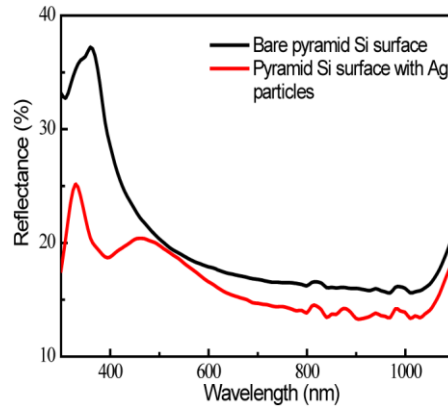


Fig. 2. Experiment results of surface reflectance curves of Si surface with different sizes of Ag nanoparticles.

As following, the influences of the size, shape and particles density distribution of Ag nanoparticles on surface reflectance were investigated in detail.

4.1 Size effect of Ag nanoparticles on surface reflectance

Through changing the sputter-anneal process conditions, Ag nanoparticles with different sizes deposited on silicon pyramid surface are obtained. And the SEM results are shown in Fig. 3(a) and 3(b). By sufficient annealing, the shapes of fabricated Ag nanoparticles are all spheroidal and their average radii are about 60 and 85 nm, respectively. The surface reflectance curves of these two samples are given in Fig. 3(c), and the predicted results by Mie theory are given in Fig. 3(d) for comparison.

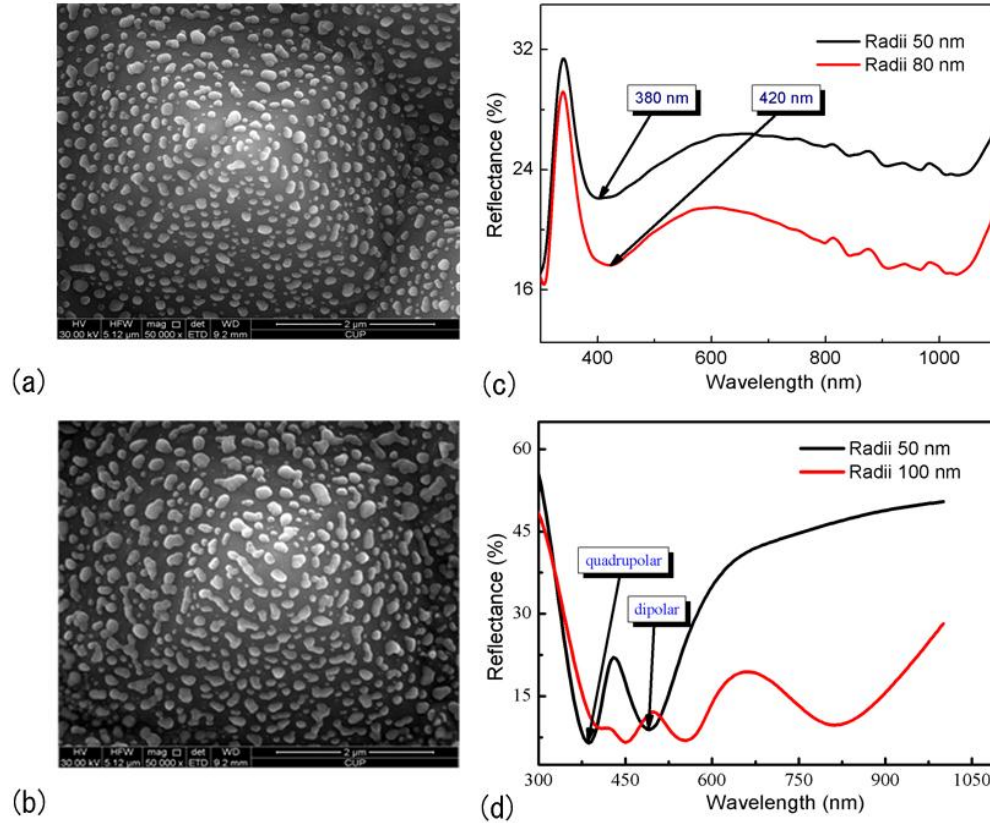


Fig. 3. Ag nanoparticles with different radii deposited on silicon pyramid surface and the surface reflectance results by experiment and calculation. (a) SEM image of silicon pyramid surface with 60 nm Ag nanoparticles deposited on the surface. (b) SEM image of silicon pyramid surface with 85 nm Ag nanoparticles deposited on the surface. (c) Experiment results of surface reflectance. (d) Calculation results of surface reflectance.

Two obvious wave troughs around 380 nm on the both reflectance curves of these two samples are observed, and this phenomenon is reappeared exactly in the calculation results. By Mie theory, these wave troughs can be attributed to the quadrupolar mode resonance of Ag nanoparticles. As the size of Ag nanoparticles increases, the slightly red-shifting from 380 to 420 nm of the wave troughs is caused by the larger relaxation time of the electrons in larger Ag nanoparticles [19,20].

Compared the two curves in Fig. 3(c), we can see that the reflectance of the sample with 85 nm Ag particles is much lower than that with 68 nm Ag particles in all frequencies range from

350 nm to 1100 nm. It is because that, as the size of Ag nanoparticles increased, higher order modes let more rays scattering forward into Si substrate. However, it doesn't mean that larger Ag particles are better, as the increased particle size can also reduce the light trapping efficiency by decreasing the scattering cross section of Ag particles. There must be an optimized size of Ag particles, which can get a trade-off between achieving higher order modes whilst suppressing the scattering cross section reduction.

4.2 Shape effect of Ag nanoparticles on surface reflectance

With insufficient annealing, there will be not enough surface tension to coalesce the flat Ag islands together for forming nanoparticles with spherical shape. In this section, we investigated particle shape effect on the reflectance of silicon pyramid surface. The SEM image of the sample and its surface reflectance curve are given in Fig. 4(b). Another curve in Fig. 4(b) is obtained from a sufficient annealed sample with the same fabricated conditions for comparison.

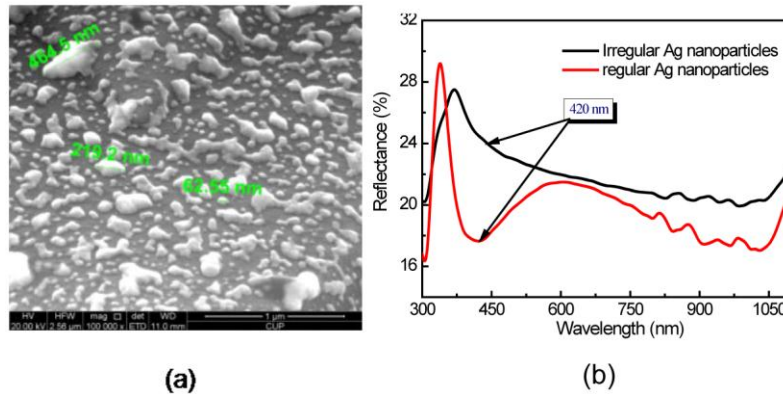


Fig. 4. SEM image of the sample with irregular particle shape Ag nanoparticles and the surface reflectance properties comparison with regular sample. (a) SEM image of sample with irregular shape Ag nanoparticles. (b) Reflectance comparison between with regular shape Ag nanoparticles and irregular shape Ag nanoparticles on the surface.

From Fig. 4(b) we can see that, the sample with irregular Ag nanoparticles obtains a higher reflectance and the wave trough of reflectance curve around 420 nm is disappeared. A reasonable explanation is that Ag nanoparticles with irregular shapes act as a homogeneous layer with an effective refractive index between Si and air. And this homogeneous layer can slightly reduce the surface reflectance [9].

4.3 The influences of particle density on surface reflectance

By adjusting the conditions of sputter-annealing process, two samples with likely particle sizes but with different particle densities were obtained on silicon pyramid surface, and their SEM images are given in Fig. 5(a) and 5(b). An obviously higher particle density can be observed in Fig. 5(a) which also contains mounts of smaller particles around the bigger ones.

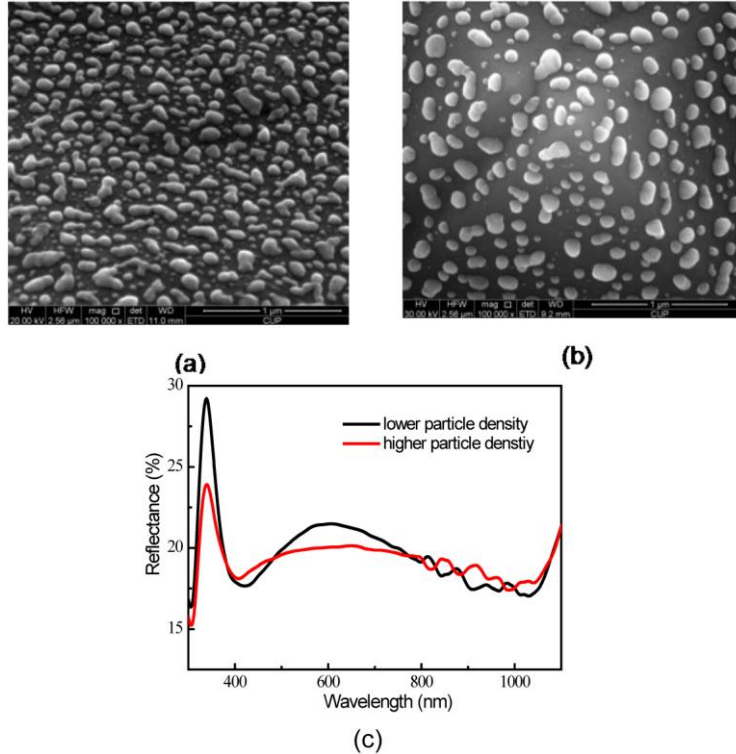


Fig. 5. SEM results and surface reflectance properties of the structure with different densities of Ag nanoparticles on the surface. (a) SEM image of sample with higher particle density. (b) SEM image of sample with smaller particles density. (c) Surface reflectance with different particle densities.

The reflectance curves of these two samples are measured and shown in Fig. 5(c), from which we can see that the sample with higher Ag particles density shows much lower reflectance on both sides of the wave trough positions around 420 nm, which corresponding to the quadrupolar mode resonance of Ag nanoparticles. This phenomenon probably results from the surfaces of the pyramid are covered imperfectly by the scattering cross section of Ag nanoparticles. As the scattering cross section of Ag nanoparticles associate with the frequency of incident light, when the frequencies of incident light far away from the quadrupolar mode resonance position (the wave troughs in reflectance curves), the scattering cross section of Ag nanoparticles samples with low particle density couldn't cover the whole silicon pyramid surface well [21]. While, for the sample with more Ag nanoparticles, the higher density remedies this defects and shows a lower surface reflectance.

5. Conclusions

Ag nanoparticles were fabricated on silicon pyramid surface by sputter-anneal process, and the surface reflectance of this structure has been studied. Compared with the bare silicon pyramid surface, the surface reflectance around 380 nm shows a dramatic reflectance reduction. By theoretical simulations based on Mie theory and experimental researches, the reflectance reduction mechanisms of this structure were investigated and the influences of several factors on the reflectance were studied systematically. Within certain range of size, an obvious decrease of the surface reflectance could be obtained as the sizes of Ag nanoparticles increase. But when their sizes greater than a certain value, the surface reflectance would increase instead owing to the reduction of their scattering cross section. Ag nanoparticles with irregular shapes show a weak anti-reflectance effect, since in this situation, they play a role more like a

homogeneous layer with an effective refractive index. Lower Ag particles density will lead to higher surface reflectance for the light with frequencies on both sides of the wave trough positions as the surfaces of the pyramid are covered imperfectly by the scattering cross section of Ag nanoparticles. For the sample fabricated by optimized process, the largest total reflectance reduction about 3.4% was achieved when the silicon pyramid surface is 35% covered by spherical Ag nanoparticles, whose average radii around 68 nm.

As a conclusion, the new structure proposed with proper particle sizes, regular shapes and higher densities of Ag nanoparticles could be adopted to reduce the surface reflectance for silicon pyramid. These results also show a practicable method to improve the light trapping efficiency for other textured surfaces.

Acknowledgment

We acknowledge support by the National Natural Science Foundation of China (Grant No. 51172069), and Ph.D. Programs Foundation of Ministry of Education of China (20110036110006), and the Fundamental Research Funds for the Central Universities (Key project 11ZG02).